

Visual observation of dispirations in liquid crystals

Yoichi Takanishi, Hideo Takezoe, and Atsuo Fukuda

Tokyo Institute of Technology, Department of Organic and Polymeric Materials, O-okayama, Meguro-ku, Tokyo 152, Japan

Junji Watanabe

Tokyo Institute of Technology, Department of Polymer Chemistry, O-okayama, Meguro-ku, Tokyo 152, Japan

(Received 25 October 1991)

In this work, wedge-screw and twist-edge dispirations in liquid crystals were visually observed. In smectic phases, such as the antiferroelectric SmC_A and the dimeric SmC_2 , where the molecules or the mesogenic groups in the adjacent smectic layers tilt in opposite senses, we found the schlieren texture with the strength of $m = \pm \frac{1}{2}$ which should not be seen in the normal SmC phase. The observation indicates the existence of a wedge-screw dispiration; i.e., a π -wedge disclination ($m = \frac{1}{2}$) accompanied by a screw dislocation that is characterized by the Burgers vector \mathbf{b} whose magnitude is equal to the layer thickness d . A threadlike defect line with $\pm\pi$ -wedge disclinations at the ends observed in freely suspended films manifests a twist-edge dispiration; i.e., a linked structure of a π -twist disclination and a $|\mathbf{b}|=d$ edge dislocation.

INTRODUCTION

Various defects may be observed in liquid crystals. Disclinations, such as a schlieren texture¹ and a thread line, are commonly observable in nematic cells. Because of a liquidlike disorder in the center of gravity of the molecules, a dislocation does not appear in the nematic phase. Since the smectic-*A* (SmA) phase may be considered as a one-dimensional solid, we can make a dislocation topologically, whose energy is proportional to the square of the Burgers vector.² In the SmC phase, a disclination is commonly observed in addition to the dislocation because of the existence of the \hat{C} director, i.e., the projection of molecules onto the smectic plane.

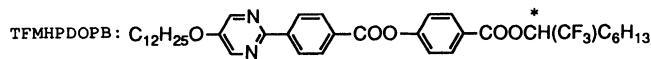
In chiral tilted smectic phases, such as the SmC^* phase, the creation of dislocations should be accompanied by the appearance of disclinations because of the existence of a helical structure. The Frank vector of the disclination is $q\mathbf{b}$, where q is the wave number of the helix and the Burgers vector \mathbf{b} has a magnitude equal to the layer thickness d . Such a linear defect accompanying a dislocation and a disclination is called a dispiration.^{3,4} Using the theoretical expression of the elastic energy of a screw dislocation in the SmC phase,⁵ Lejcek^{6,7} considered the energy of the basic property of the dispiration in the SmC^* phase. However, to date the dispiration has not actually been observed in the SmC^* phase, since the Frank vector $q\mathbf{b}$ is too small for the disclination to be seen. Though the dispiration itself was considered topologically by Harris³ in 1970, it has scarcely been reported even in normal crystals⁸ and polymers.⁹

In this paper, we report direct observation of various textures in the SmC_A (Ref. 10) and the SmC_2 (Ref. 11) phases and the visual confirmation of the dispirations in these phases; from the structural point of view, the observation of the schlieren texture of the strength $m = \pm \frac{1}{2}$ ($\pm\pi$ disclination) in these phases indicates the existence of accompanying screw dislocations, namely, a wedge-screw dispiration. The existence of a twist-edge dispiration is also confirmed, based on the texture of the freely suspended films. We note that these are direct visual observations of dispirations in liquid crystals.

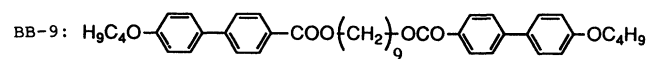
tion is also confirmed, based on the texture of the freely suspended films. We note that these are direct visual observations of dispirations in liquid crystals.

EXPERIMENTAL PROCEDURE

Samples used were racemate of TFMHPDOPB (Refs. 12 and 13) and BB-9 (Ref. 14), whose chemical structures and phase (and transition-temperature) sequences are as follows:



Iso. 110 °C SmA 96.8 °C SmC 69.5 °C SmC_A 43 °C Cryst.



Iso. 125 °C SmC_2 80 °C Cryst.

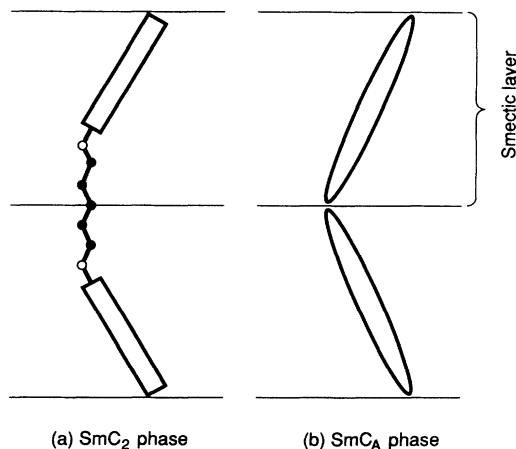


FIG. 1. Schematic illustration of (a) the molecular structure of BB-9 and (b) molecular arrangement in SmC_A .

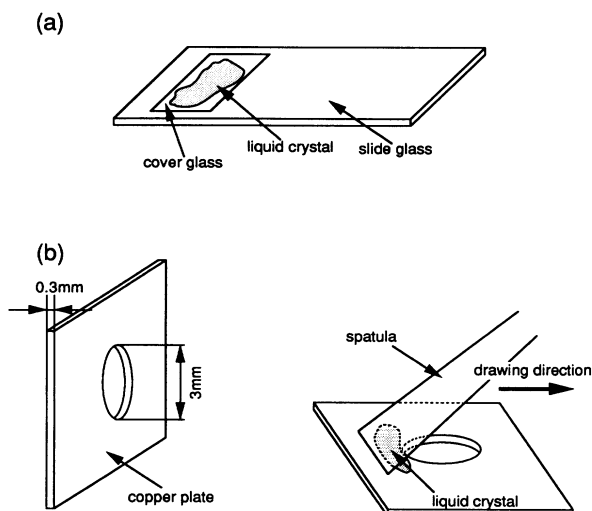


FIG. 2. Structures of sample cells, (a) sandwich cell and (b) freely suspended film cell.

The reason for choosing these two materials is as follows. Since the racemate of TFMHPDOPB undergoes the first-order SmA - SmC phase transition,¹³ the resultant large tilt angle in SmC and SmC_A makes the observation of the defects of the \hat{C} director much easier because of the large optical birefringence in these tilted phases. As for BB-9, an x-ray-diffraction measurement verifies the zig-zag (anticlinic) structure, where two mesogenic groups

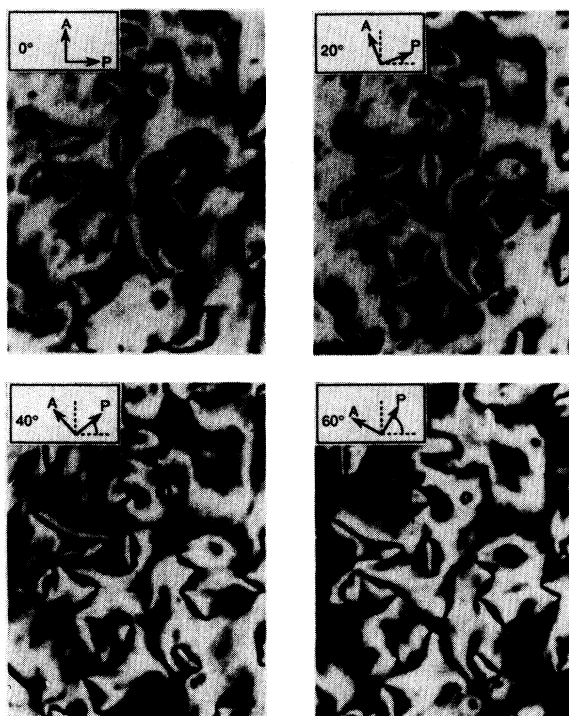


FIG. 3. Optical micrographs ($\times 200$) of BB-9 in SmC_2 in a sandwich cell taken while rotating the crossed polarizers counterclockwise. Note the presence of $\pm\pi$ disclinations with two dark brushes.

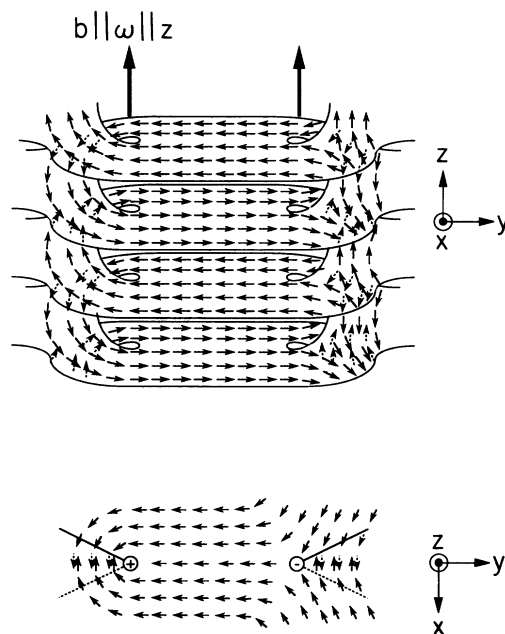


FIG. 4. Structure of a screw-wedge dispiration. The arrow indicates the \hat{C} director, the projection of the director onto the smectic plane. The screw dislocation line and the wedge disclination line are along the layer normal (z axis) with the Burgers vector $\mathbf{b}=(0,0,d)$ and the Frank vectors $\boldsymbol{\omega}=(0,0,\pm\pi)$, respectively.

tilt in opposite senses [Fig. 1(a)],¹¹ in a similar fashion to that in SmC_A [Fig. 1(b)].¹⁰

We prepared two types of sample cells. One was a sandwich cell [Fig. 2 (a)]. A thin sample liquid crystal was sandwiched between a micro-slide-glass plate and a micro-cover-glass without spacer. BB-9 sample was sheared off slightly in order to be aligned homeotropically. The other was a freely suspended film¹⁵ [Fig. 2 (b)]. We used a 0.3-mm-thick copper plate with a hole of 3-mm diameter, heated the sample at the edge of the hole into the SmA or SmC_2 phases, and pulled it across the hole with a spatula as a spreader. In both the sample cells, liquid crystals were aligned homeotropically, so that the smectic layer was parallel to the plates. The texture observation was made under a polarizing microscope (Nikon OPTIPHOT-POL) using objective ($4\times, 20\times, 40\times$). The temperature of the cells was controlled by a Mettler FP82. The sign of defects was determined by the rotation sense of dark brush lines of the

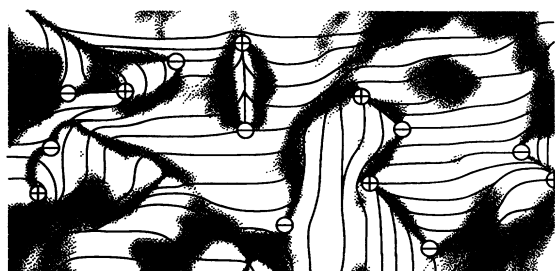


FIG. 5. \hat{C} -director orientation corresponding to Fig. 3.

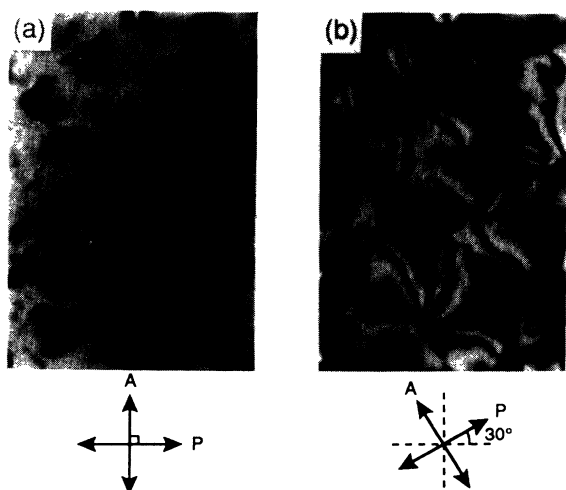


FIG. 6. Optical micrographs ($\times 200$) of BB-9 in the SmC_2 phase in a sandwich cell. (a) Six brushes showing a 3π disclination. (b) Six brushes appear to consist of groups of four and two lines when the crossed polarizers are rotated by 30° .

schlieren texture when we rotated a polarizer and an analyzer, keeping the crossed polarizers.

RESULTS AND DISCUSSION

It is well known, in tilted smectic phases such as SmC , that the schlieren textures of the same kind as in the nematic (N) phase are observable in homeotropically aligned cells due to the distribution of the \hat{C} director. However, there exists an essential difference between these in the N and SmC phases; the strength of the defects is generally restricted to $m = \pm 1$, and $\pm\pi$ disclinations ($m = \pm\frac{1}{2}$) cannot exist in the SmC phase, since they cause the nucleation of discontinuous defect planes due to the discrepancy between the tilting senses in SmC , while not only $\pm 2\pi$ but also $\pm\pi$ disclinations exist in the N phase.

Figure 3 shows the schlieren texture of BB-9 in the SmC_2 phase in a sandwich cell taken as crossed polarizers rotated counterclockwise. When observed carefully,

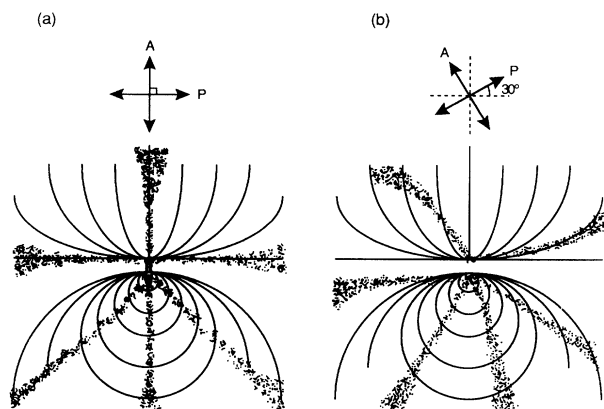


FIG. 7. \hat{C} -director orientation corresponding to Fig. 6.

there exist points from which two dark brushes come out. These points are $\pm\pi$ -wedge disclinations similar to those seen in nematic cells. For the existence of the $\pm\pi$ disclinations, the discontinuous defect planes due to the discrepancy between the tilting senses should have somehow been removed. The removal is easily attained in the SmC_2 phase, where two mesogenic groups of one molecule tilt in opposite senses from the layer normal in the adjacent smectic layers, as shown in Fig. 1(a). In such a layer structure, the discontinuous plane perpendicular to the layer can be removed by creating a screw dislocation along the disclination line. The dislocation

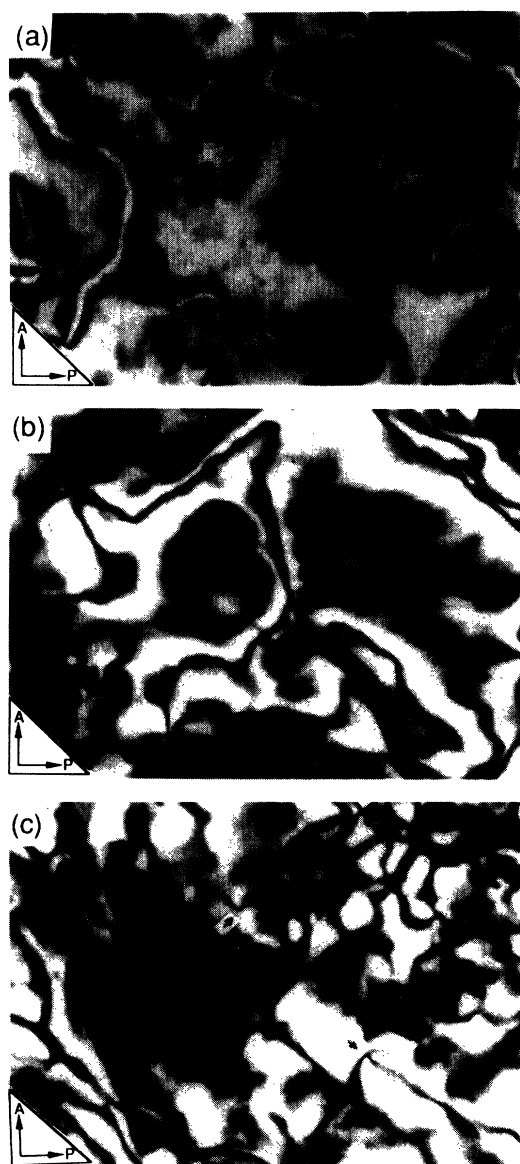


FIG. 8. Optical micrographs ($\times 200$) of the racemic TFMHPDOPB in the SmC and SmC_A phases in a sandwich cell. (a) In the SmC phase, only four brushes which show $\pm 2\pi$ disclinations are observed. (b) In the SmC_A phase, a loop showing inversion wall is observed. It may shrink or expand with rotation of the crossed polarizers. (c) In another SmC_A -phase region, two brushes which show $\pm\pi$ disclinations are observed.

line along the smectic layer normal z is characterized by the Burgers vector $\mathbf{b}=(0,0,d)$, where d is the layer thickness. Thus $\pm\pi$ disclinations can exist as well as $\pm 2\pi$ disclinations in the SmC_2 phase. The structure of the $\pm\pi$ disclination in the SmC_2 phase is illustrated in Fig. 4, where the $\hat{\mathbf{C}}$ directors are shown by arrows to distinguish the tilt sense. This is exactly the wedge-screw dispiration, i.e., a linked structure of a screw dislocation of the Burgers vector $\mathbf{b}=(0,0,d)$ and one of $\pm\pi$ -wedge disclinations of the Frank vector $\omega=(0,0,\pm\pi)$. The observation of the schlieren textures with two brushes proves the existence of the wedge-screw dispiration.

Considering the rotational senses of the brushes when the polarizer and the analyzer are rotated with their relative (crossed) orientation kept fixed, the $\hat{\mathbf{C}}$ director in this photograph (Fig. 3) is drawn, as illustrated in Fig. 5; defects with the opposite signs are connected alternately.

In the SmC_2 phase, the schlieren texture with six brushes is also observed, as shown in Fig. 6(a). This indicates the existence of a 3π disclination ($m=\frac{3}{2}$) as illustrated in Fig. 7, which is regarded as a kind of combined structure of π and 2π disclinations. By carefully observing the rotational sense of the brushes and the point from which six brushes come out as the polarizers are rotated, we notice that the sign of the defect is positive and that the point occasionally separates into two, from which four and two lines may exit, as shown in Fig. 6(b). Therefore, the $+2\pi$ -wedge disclination and the wedge-screw dispiration ($+\pi$ -wedge disclination and $|\mathbf{b}|=d$ screw dislocation) seem to separate but remain close to each other, as shown in Fig. 7(b). The reason of the preferential attractive force between these two defects of the same sign is not known as yet.

Figure 8(a) shows the texture of racemic TFMHPDOPB in the SmC phase in a homeotropically aligned sandwich cell. For the reason stated above, only the $\pm 2\pi$ disclinations appear in the large area of about 50 mm^2 and no $\pm\pi$ disclination is observed. When the temperature was decreased so that a transition to the SmC_A phase occurred, the texture changed violently. Note the appearance of two kinds of defects: One is a loop, as



FIG. 9. $\hat{\mathbf{C}}$ -director orientation corresponding to Fig. 8(b).

shown in Fig. 8(b); and the other is a point with two brushes, as shown by the arrows in Fig. 8(c). The former is an inversion wall, whose $\hat{\mathbf{C}}$ -director orientation is illustrated in Fig. 9, and the latter is the same as the one observed in the SmC_2 phase. Thus we found the wedge-screw dispiration also in the SmC_A phase. Conversely, it is important to notice that the observation of the schlieren texture of $m=\pm\frac{1}{2}$ as in Figs. 3 and 8(c) pro-

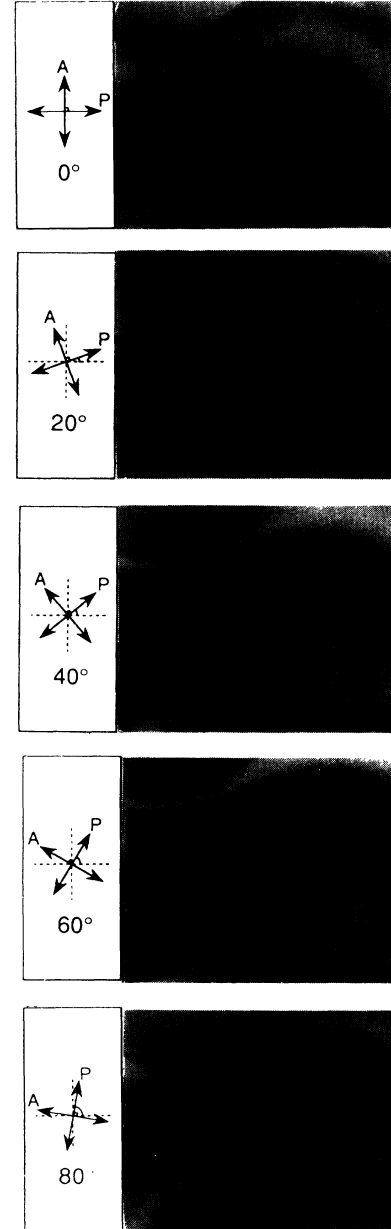


FIG. 10. Series of optical micrographs ($\times 65$) of racemic TFMHPDOPB in the SmC_A phase in a freely suspended film, which were taken as rotating the crossed polarizers counterclockwise by 20° increments. Threadlike line defects with brushes at their ends are observed, showing wedge-screw dispirations and twist-edge dispirations (see text).

vides a simple and reliable method to confirm the presence of the SmC_A or the SmC_2 phase.¹⁶

In the texture observation shown in Figs. 3 and 8, the probability of finding $\pm\pi$ disclinations in the SmC_A phase seems to be less than that in the SmC_2 phase. The stability of the dispiration must be related to the stability of the dislocation in the local zigzag structure. In this sense, the SmC_2 phase of BB-9, where only one molecule can construct anticlinic layer structure, supplies much more favorable conditions for the appearance of the dispiration than the SmC_A phase, where pairing of two molecules is responsible for the anticlinic structure.¹⁷ Since the pairing is dynamical, the layer structure of SmC_A is less firmly established and hence the dislocation may more easily relax as compared with that in the SmC_2 phase. We are measuring higher-order x-ray diffraction due to the layer structures in these phases in order to clarify the difference in these layer structures. The results will be reported in the future.

Interesting textures were also observed in SmC_A of freely suspended films of TFMHPDOPB as shown in Fig. 10. By rotating a set of crossed polarizers counterclockwise, we took a series of optical micrographs at every 20°. Threadlike lines together with brushes are characteristic features. A simple line defect without branches is attributed to an edge dislocation line parallel to the smectic layer and with the Burgers vector $\mathbf{b}=(0,0,d)$. The brush rotation senses indicate that $\pm\pi$ -wedge disclinations are located at both its ends. Consequently, the existence of the two wedge-screw dispirations at the ends of the line is necessarily concluded. Moreover, since the \hat{C} directors in two adjacent layers with the edge dislocation orient to the opposite senses, the dislocation is accompanied by a π -twist disclination with the Frank vector $\omega=(0,0,\pi)$. This confirms the existence of the twist-edge dispiration

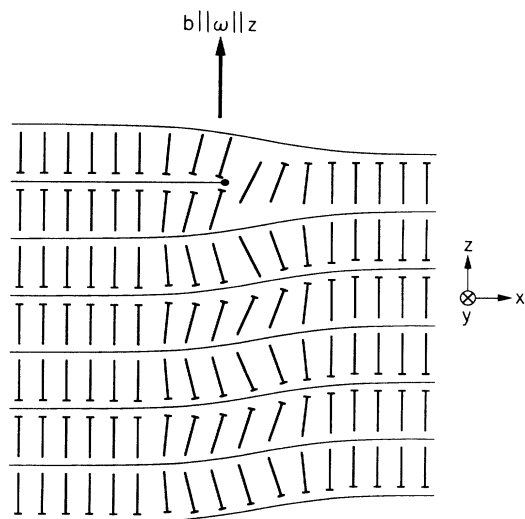


FIG. 11. Structure of a twist-edge dispiration. The projection of the directors onto the plane parallel to the layer normal is expressed by T shapes. The edge dislocation line and the twist disclination lines lie along the layer plane (y axis) with the Burgers vector $\mathbf{b}=(0,0,d)$ and the Frank vector $\omega=(0,0,\pi)$, respectively.

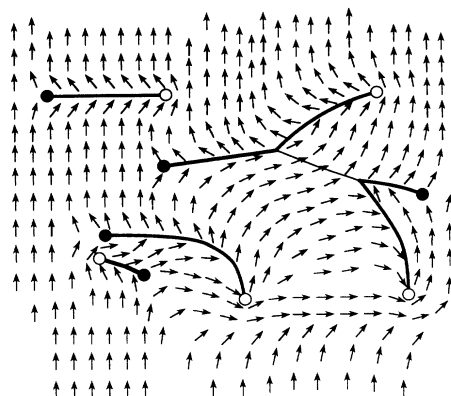


FIG. 12. \hat{C} -director orientation around the defect illustrated in Fig. 10. Open and closed circles represent $+\pi$ and $-\pi$ disclinations, respectively, and no disclination exists at the branching points. Thick and thin solid lines are edge dislocations whose Burgers vectors are odd and even multiples of d in magnitude, respectively.

as shown in Fig. 11, where the projection of the directors onto the plane parallel to the layer normal is denoted by T shapes to distinguish the tilt sense. The figure shows an intersection perpendicular to the edge dislocation line (along the y axis) and parallel to the screw dislocation line (along the z axis). Thus, the edge dislocation of nanometer in core diameter is visualized by decorating it with the twist disclination of micrometer in core diameter.

Figure 12 is a \hat{C} -director map deduced by carefully analyzing the photographs of Fig. 10. Open and closed circles represent $+\pi$ and $-\pi$ disclinations, respectively, and no disclination exists at the branching points. Thick and thin lines are edge dislocations whose Burgers vectors are odd and even multiples (probably 1 and 2) of d in magnitude, respectively. Note that the thick line separates the \hat{C} -director fields of the opposite senses, while the senses of the \hat{C} -director fields are the same in the regions separated by a thin line. Therefore, at least thick lines represent the twist-edge dispiration characterized by Frank vectors $\omega=(0,0,+\pi)$ and the Burgers vector $\mathbf{b}=(0,0,d)$. If the thin line possesses a twist disclination with the strength of $m=\pm$ integer, this line is also the twist-edge dispiration characterized by Frank vectors $\omega=(0,0,2m\pi)$ and the Burgers vectors $\mathbf{b}=(0,0,2md)$.

Figure 13(a) is an inversion wall observed in a thicker freely suspended film of the same sample. The \hat{C} -director

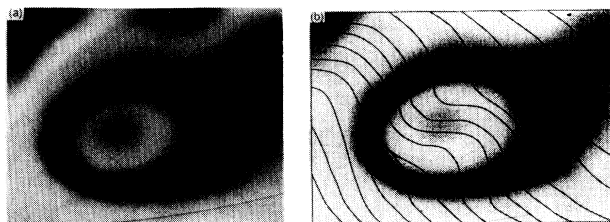


FIG. 13. (a) Inversion wall observed in an optical micrograph ($\times 65$) of racemic TFMHPDOPB in the SmC_A phase in a freely suspended film, and (b) the corresponding \hat{C} -director orientation.

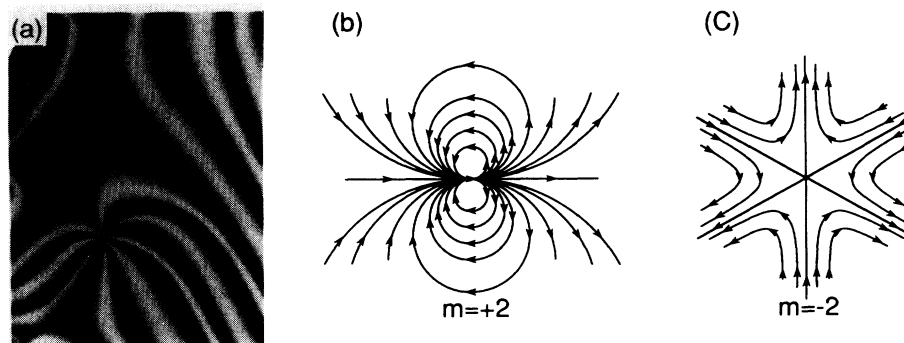


FIG. 14. (a) Optical micrograph ($\times 65$) of racemic TFMHPDOPB in the SmC_A phase in a freely suspended film. An eight-brush defect showing a 4π disclination is seen. The \hat{C} -director orientations corresponding to (b) $+4\pi$ disclination and (c) -4π disclination.

orientation of the inversion wall, the same as Fig. 8(b), is illustrated in Fig. 13(b). An eight-brush-line defect indicating the presence of a $+4\pi$ or -4π disclination is also observed, as shown in Fig. 14(a). The \hat{C} -director field of $\pm 4\pi$ disclinations is shown in Figs. 14(b) and 14(c), respectively, which have a combined structure of two $+2\pi$ or -2π disclinations. Whether or not the occurrence of the defect with such high strength is correlated with the SmC_A phase is under investigation.

SUMMARY

By observing schlieren textures in homeotropic cells and freely suspended films of SmC_A and SmC_2 , wedge-screw and twist-edge dispirations were visually recognized. The confirmation of the wedge-screw dispiration

is based on the observation of the schlieren texture of $m = \pm \frac{1}{2}$, which should not exist in the normal SmC phase. The anticlinic director orientation from layer to layer with a screw dislocation compensates the discrepancy in the \hat{C} -director senses in $\pm\pi$ disclinations. The $|\mathbf{b}|=d$ edge dislocation identified in freely suspended films necessarily implies the existence of the $\pm\pi$ -twist disclination, indicating the presence of a twist-edge dispiration.

ACKNOWLEDGMENTS

The authors acknowledge Dr. L. Lejcek of Czechoslovakia Academy of Sciences for comments on the subject of dispirations. Their thanks are due to Mitsubishi Petrochemical Co. Ltd. for supplying the TFMHPDOPB used in this work.

- ¹D. Demus and L. Richter, *Textures of Liquid Crystals* (Verlag Chemie, Weinheim, 1978).
- ²P. G. de Gennes, *The Physics of Liquid Crystals* (Clarendon, Oxford, 1974).
- ³W. F. Harris, *Philos. Mag.* **22**, 949 (1970).
- ⁴M. Kléman, *Points, Lines and Walls* (Wiley, New York, 1983).
- ⁵M. Kléman and L. Lejcek, *Philos. Mag. A* **42**, 671 (1980).
- ⁶L. Lejcek, *Czech. J. Phys. B* **35**, 726 (1985).
- ⁷L. Lejcek, *Czech. J. Phys. B* **34**, 563 (1984).
- ⁸F. Reynaud and A. Ben Lamine, *Acta Metall.* **29**, 1485 (1981).
- ⁹D. H. Reneker and J. Mazur, *Polymer* **24**, 1387 (1983).
- ¹⁰A. D. L. Chandani, E. Gorecka, Y. Ouchi, H. Takezoe, and A. Fukuda, *Jpn. J. Appl. Phys.* **28**, L1265 (1989).
- ¹¹J. Watanabe and M. Hayashi, *Macromolecules* **22**, 4083 (1989).

- ¹²S. Inui, S. Kawano, M. Saito, H. Iwane, Y. Takanishi, K. Hiraoka, Y. Ouchi, H. Takezoe, and A. Fukuda, *Jpn. J. Appl. Phys.* **29**, L987 (1990).
- ¹³A. Ikeda, Y. Takanishi, H. Takezoe, A. Fukuda, S. Inui, S. Kawano, M. Saito, and H. Iwane, *Jpn. J. Appl. Phys.* **30**, L1032 (1991).
- ¹⁴J. Watanabe and S. Kinoshita, *J. Phys. (Paris)* (to be published).
- ¹⁵R. Pindak and D. Moncton, *Phys. Today* **35**(5), 57 (1982).
- ¹⁶Y. Takanishi, H. Takezoe, A. Fukuda, H. Komura, and J. Watanabe, *J. Mater. Chem.* (to be published).
- ¹⁷Y. Takanishi, K. Hiraoka, V. K. Agrawal, H. Takezoe, A. Fukuda, and M. Matsushita, *Jpn. J. Appl. Phys.* **30**, 2023 (1991).

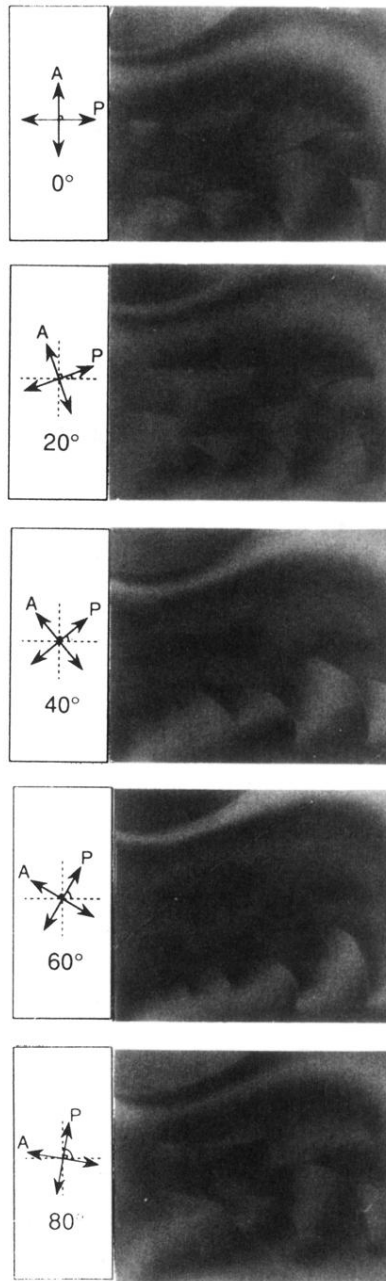


FIG. 10. Series of optical micrographs ($\times 65$) of racemic TFMHPDOPB in the SmC_A phase in a freely suspended film, which were taken as rotating the crossed polarizers counterclockwise by 20° increments. Threadlike line defects with brushes at their ends are observed, showing wedge-screw dispirations and twist-edge dispirations (see text).

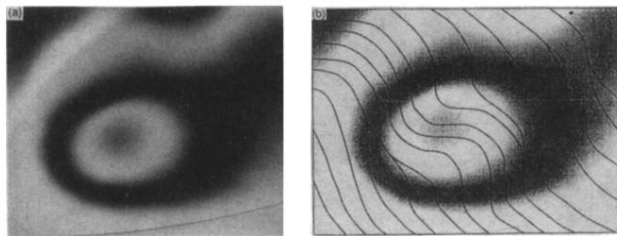


FIG. 13. (a) Inversion wall observed in an optical micrograph ($\times 65$) of racemic TFMHPDOPB in the SmC_A phase in a freely suspended film, and (b) the corresponding \hat{C} -director orientation.

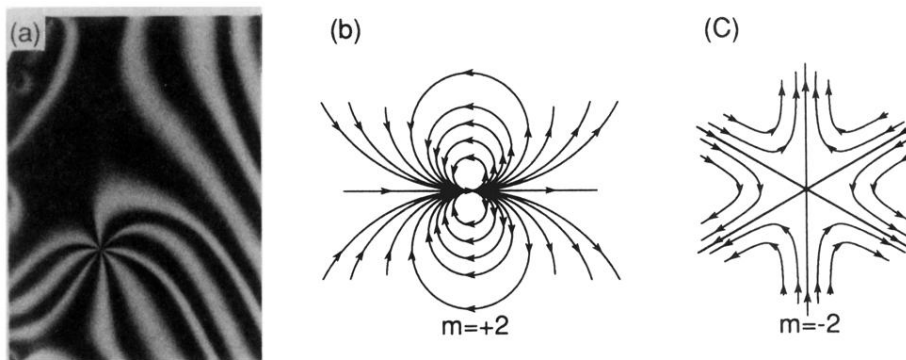


FIG. 14. (a) Optical micrograph ($\times 65$) of racemic TFMHPDOPB in the SmC_A phase in a freely suspended film. An eight-brush defect showing a 4π disclination is seen. The \hat{C} -director orientations corresponding to (b) $+4\pi$ disclination and (c) -4π disclination.

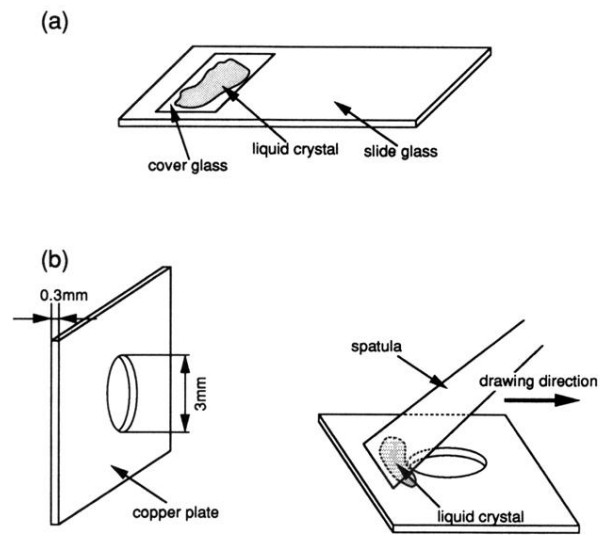


FIG. 2. Structures of sample cells, (a) sandwich cell and (b) freely suspended film cell.

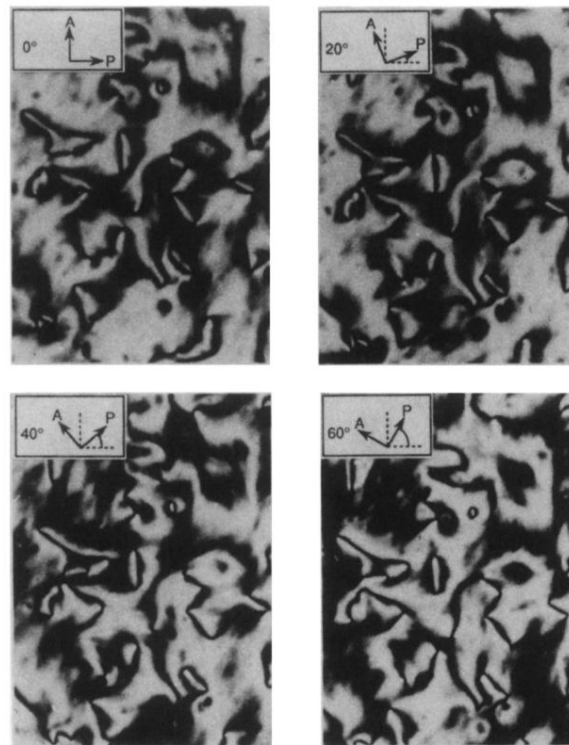


FIG. 3. Optical micrographs ($\times 200$) of BB-9 in SmC_2 in a sandwich cell taken while rotating the crossed polarizers counterclockwise. Note the presence of $\pm\pi$ disclinations with two dark brushes.

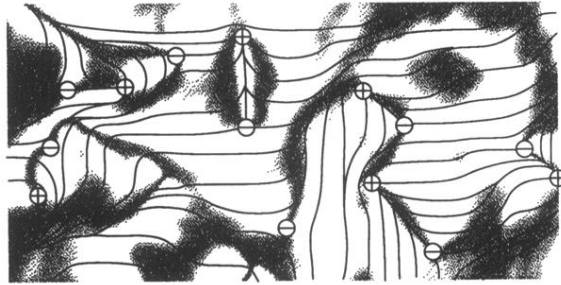


FIG. 5. \hat{C} -director orientation corresponding to Fig. 3.

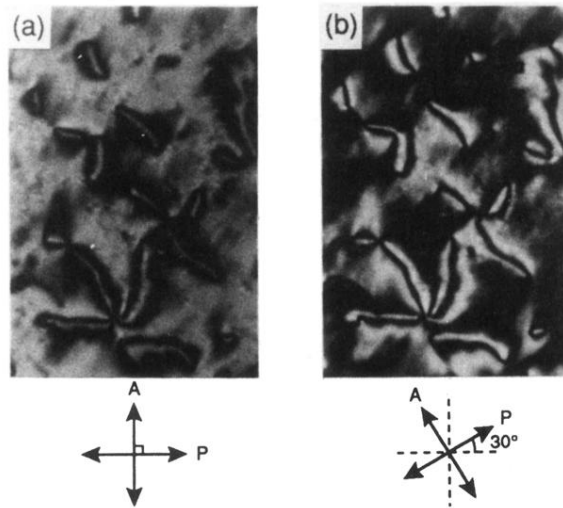


FIG. 6. Optical micrographs ($\times 200$) of BB-9 in the SmC_2 phase in a sandwich cell. (a) Six brushes showing a 3π disclination. (b) Six brushes appear to consist of groups of four and two lines when the crossed polarizers are rotated by 30° .

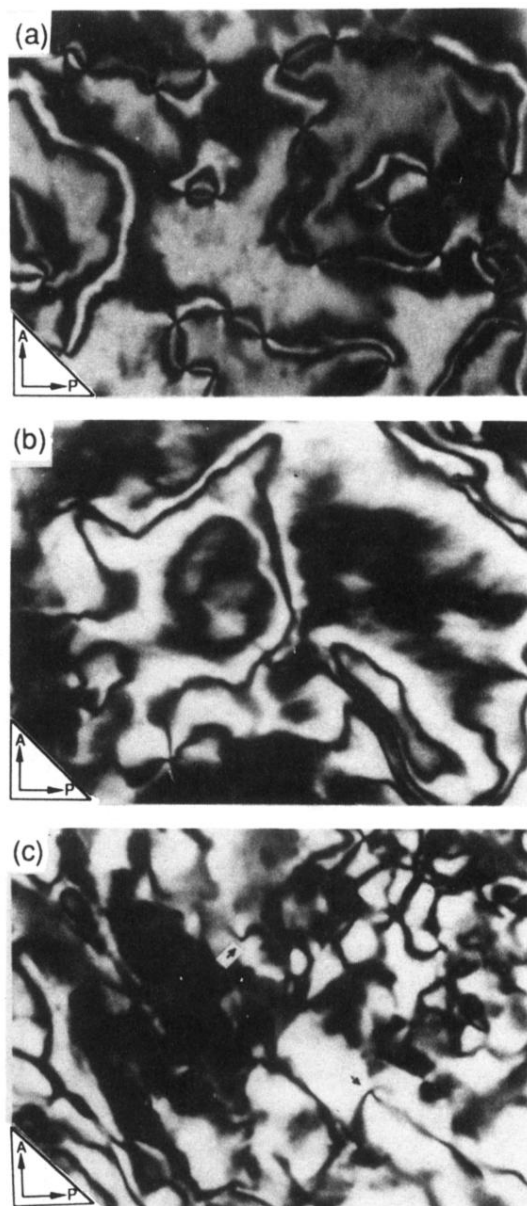


FIG. 8. Optical micrographs ($\times 200$) of the racemic TFMHPDOPB in the SmC and SmC_A phases in a sandwich cell. (a) In the SmC phase, only four brushes which show $\pm 2\pi$ disclinations are observed. (b) In the SmC_A phase, a loop showing inversion wall is observed. It may shrink or expand with rotation of the crossed polarizers. (c) In another SmC_A -phase region, two brushes which show $\pm \pi$ disclinations are observed.

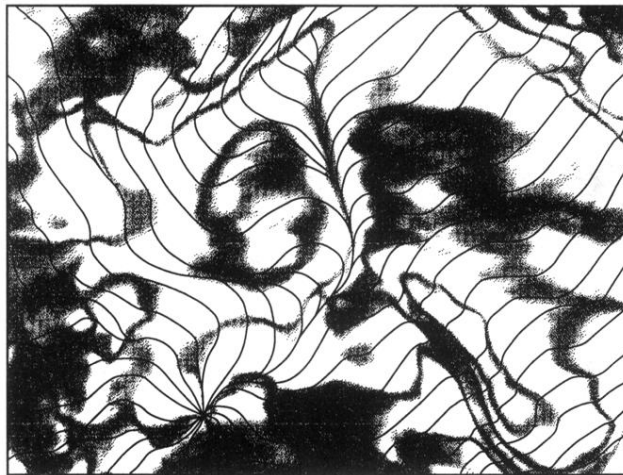


FIG. 9. \hat{C} -director orientation corresponding to Fig. 8(b).